# Enhancing performance of tuned mass dampers in mitigating seismic response of nonlinear structures

Amir Hossein Jafarieh*, Saina Ebrahimnia

Department of Civil Engineering, Faculty of Engineering and Technology, University of Mazandaran, Babolsar, Iran.

**Abstract:**

Tuned mass dampers (TMDs) are widely used to mitigate seismic vibrations. However, studies have shown that TMD effectiveness diminishes in nonlinear systems and varies under different ground motions. This study investigates TMD performance in elastic and inelastic single-degree-of-freedom (SDOF) and multi-degree-of-freedom (MDOF) structures. Numerical models were constructed in OpenSees and subjected to 20 ground motion records. A parametric analysis examined the influence of TMD stiffness on displacement and inter-story drift using nonlinear time history analysis. The TMD stiffness ratio was systematically varied to identify an optimal value that maximizes response mitigation in nonlinear systems. Results indicate that traditional TMDs, tuned to the structure's fundamental frequency, often underperform in nonlinear systems. In some cases, they may amplify responses at higher ductility levels. For SDOF systems, reducing TMD stiffness below traditional values noticeably improves performance. Optimal TMD stiffness was determined by minimizing displacement ratios. For MDOF structures, reducing TMD stiffness below the traditional value decreases the response ratio in the upper stories of elastic structures and in all stories of inelastic structures. Notably, optimal TMDs selected by minimum total story displacement ratios differed from those selected by minimum inter-story drift ratios. This improved stiffness-based tuning strategy was subsequently applied to a Tuned Structural Mass Damper (TSMD) for nonlinear systems. The TSMD utilizes a portion of existing roof mass, thereby eliminating the need for additional weight. For SDOF systems, the TSMD demonstrated considerably better performance. In MDOF systems, TSMDs reduced inter-story drifts in inelastic structures and mitigated drift amplification in upper floors.

**Keywords:** TMD, SDOF, MDOF, Ductility, Drift.

## 1. Introduction

* Corresponding author's email: ah.jafarieh@umz.ac.ir

Seismic resilience of buildings has been a longstanding concern in structural engineering, leading to the development of various vibration control strategies. Among these, tuned mass dampers (TMDs) have emerged as a promising solution for controlling and reducing the dynamic response of structures. Traditional TMDs are passive control devices consisting of a mass, a spring, and a damping system, typically tuned to the natural frequency of the structure to counteract its vibrations. The concept of TMDs dates back to the early 20th century, when Frahm first proposed using a secondary mass to reduce vibrations in mechanical systems [1]. Over the years, researchers have pursued various strategies to improve the performance of TMDs. The existing body of research can be organized into five distinct categories, as follows:

The first category encompasses foundational and classical TMD theory. Den Hartog developed foundational theories for optimizing TMD parameters [2]. McNamara studied the use of TMDs in civil engineering, particularly for mitigating wind-induced vibrations in tall buildings [3].

In the second category, researchers have attempted to optimize conventional TMDs to achieve better performance. For instance, Den Hartog [2] provided the closed-form formulas for calculating the optimal tuning frequency and optimal damping ratio of a TMD to minimize the vibration of the primary system. Sadek et al. [4] proposed a systematic method for estimating the optimal parameters of tuned mass dampers (TMDs) specifically for seismic applications, considering the characteristic properties of earthquake ground motions. Their approach provides practical design formulas that account for the non-stationary nature of seismic excitation, offering an alternative to classical Den Hartog optimization, which was originally developed for steady-state harmonic loads. Warburton [5] presented a comprehensive framework for determining optimum tuned mass damper parameters across a wide range of excitation types, including harmonic, white noise, and seismic excitations, as well as various response measures such as displacement, acceleration, and force. This work significantly extended earlier optimization theories by providing closed-form solutions for different combinations of excitation and response parameters. Leung and Zhang [6] applied a particle swarm optimization (PSO) algorithm to determine the optimal parameters of tuned mass dampers for structures subjected to seismic excitations. Zhang and Zhang [7] studied the effect of an optimal TMD on a tall intake tower used in hydraulic applications. Their results showed a considerable effect of the TMD, especially when higher mass ratios were used. Etedali et al. [8] proposed the FTMD concept. They combined a traditional TMD with a friction damper and evaluated the optimal seismic control performance of TMDs and FTMDs in high-rise buildings under near-fault earthquakes. Their analyses also accounted for soil-structure interaction (SSI) effects. Love et al. [9] evaluated two full-scale high-rise buildings, one equipped with a TMD, under three wind events. In that study, two identical TMDs were installed in a super-tall building. Araz [10] studied a T-TMD system consisting of two spring elements, one damping element, and a mass. They showed that the proposed system is generally effective in reducing structural response under harmonic excitations. Ozturk et al. [11] proposed an optimal placement height using an optimization method. They also employed an effective design approach to simultaneously determine the parameters of multiple tuned mass dampers (MTMDs). The objective was to reduce the seismic response of a multi-story shear building. Jafarinia and Ostad-Ali-Askari [12] used an optimization algorithm to design MTMD parameters for structural response reduction. Khatibinia et al. [13] employed two optimization methods to design TMD parameters to reduce damage indices.

Within this category, some researchers have focused on finding the optimal placement of TMDs. As mentioned earlier, Ozturk et al. [11] proposed an optimal placement height using an optimization method, along with an effective design approach to determine optimal MTMD parameters. Kontoni and Farghaly [14] investigated different scenarios for TMD placement in plan and elevation for two geometrically and vertically irregular high-rise structures. Their results indicated that placing TMDs in the upper half of the structure significantly reduced seismic responses, and soil-structure interaction was included in their analyses.

The studies in the third category propose novel TMD designs. Lu et al. [15] proposed a type of damper called a particle damper (PD). The suggested system consists of metal balls placed inside a box, where the balls are free to move within the box. Wu et al. [16] introduced the idea of a magnetic TMD that generates a nonlinear repulsive force. The system is capable of reducing seismic oscillations over a wide frequency range. Kang and Peng [17] identified optimal parameters for high-mass-ratio TMDs using numerical optimization methods. Their results revealed notable effectiveness of TMDs with large mass ratios. De Angelis et al. [18] proposed the idea of a ground-connected linear inerter and optimized its parameters. This system provides increased inertia for the TMD without requiring additional mass. Lara-Valencia et al. [19] designed an optimized TMDI using a comprehensive optimization process. Gao et al. [20] noted that conventional TMDs with fixed frequencies do not perform well under ground motions having various frequency contents. They proposed a TMD called FATMD, which can be tuned to the excitation frequency. Masnata et al. [21] investigated hybrid control systems such as TMDI and base isolation under seismic excitation. They optimized the TMDI parameters. Araz [22] proposed a method for optimizing TMDI parameters to reduce maximum structural responses in high-rise buildings subjected to earthquakes. They also investigated the effect of SSI on dynamic responses and optimal TMDI parameters. Besharatian et al. [23] designed an optimized frictional TMD (FTMD). They examined three different mass ratios based on previous studies. Das et al. [24] investigated the application of an optimized TMDI in controlling structural responses under seismic and wind loads.

Additionally, within this category, some studies utilized a partial mass approach, especially for isolated structures. Sakr [25] introduced the idea of using multiple TMDs (MTMDs). They used a portion of the floor load from several stories as the TMD mass. The main advantage of this method is that it eliminates the need for the large additional masses required in traditional TMD systems. Anajafi and Medina [26] proposed a new technique called partial mass isolation (PMI) to address the shortcomings of conventional base isolation systems and TMDs. This technique isolates portions of the floor mass. Manchalwar and Bakre [27] studied the use of base isolation on the top floor as a TMD.

In the fourth category, TMDs are combined with base-isolated systems to improve performance through a hybrid approach. Stanikzai et al. [28] investigated the seismic response of several base-isolated structures equipped with a single TMD (STMD), multiple TMDs (MTMDs), and multiple TMDs distributed across floors (d-MTMD). Their results showed a significant reduction in top-floor acceleration using MTMDs and d-MTMDs. Di Matteo et al. [29] studied hybrid control systems for seismic response control of single-degree-of-freedom and multi-degree-of-freedom base-isolated structures. Three control systems were examined: two were conventional TMDs, and one was a new TMD connected to the ground via a damper.

In the fifth category, researchers have focused on the nonlinear behavior of structures. Mohammadi and Ziarani [30] conducted a numerical search to determine the optimal parameters of a TMD to reduce the maximum seismic response of a structure. Their results indicated that the optimal TMD characteristics vary for each earthquake excitation due to the different frequency content of each ground motion. Bagheri and Rahmani-Dabbagh [31] developed a new seismic control system called P-TMD by replacing the viscous damper in a TMD with an elasto-plastic spring. The results showed that the proposed system significantly reduced displacement and acceleration responses while eliminating expensive viscous dampers. Roozbahan and Turan [32] introduced a dual-spring TMD system called DSTMD and optimized it. They examined its effects on two 10-story buildings under linear behavior and extended the results to nonlinear conditions. Shahraki et al. [33] eliminated the viscous damper and added an elastoplastic spring. They introduced an optimized elastoplastic TMDI (PTMDI) and evaluated its advantages while accounting for SSI effects.

As the literature review reveals, only a limited number of studies have addressed nonlinear structural behavior, and these are often case-study efforts or rely on fundamentally altering the TMD mechanism through additional complex components. While the partial mass approach has proven practical for simplifying TMD implementation, its effectiveness in structures undergoing nonlinear seismic response has remained largely unexplored. This is a critical oversight, given that structures inevitably experience nonlinear behavior during strong earthquakes, where conventional TMD performance is known to deteriorate significantly. The present study addresses these intertwined gaps through a twofold contribution: first, it proposes a simple and practical strategy to enhance the effectiveness of traditional TMDs in controlling nonlinear structural responses by systematically optimizing their fundamental parameters, particularly stiffness; second, it extends this strategy to systems that employ a partial mass approach, thereby bridging the gap between ease of implementation and analytical realism. The study is thus positioned at the intersection of TMD optimization, partial mass design, and nonlinear structural behavior. To ensure both conceptual clarity and practical relevance, the proposed approach is validated using both equivalent SDOF and detailed MDOF structural models.

## 2. Modeling of single-degree-of-freedom structures and input excitation

In this section, the characteristics and modeling methods of SDOF models are introduced to evaluate the effectiveness of a TMD in reducing the seismic response of structures. As shown in Fig. 1(a), the structure is modeled as a single-degree-of-freedom system. The structure is considered to have a mass $m_{str}$ and stiffness $k_{str}$. The viscous damping coefficient for the structure is denoted as $c_{str}$. According to Fig. 1(b), a tuned mass damper is also considered for the same structure. The mass, stiffness, and damping of the TMD $(m_{TMD}, k_{TMD}, c_{TMD})$ are defined as proportions of the corresponding structural parameters. These ratios are represented as $m_r$, $k_r$, and $c_r$. They are expressed in the following equations.

$$m_r = m_{TMD} / m_{str} \tag{1}$$

$$k_r = k_{TMD} / k_{str} \tag{2}$$

$$c_r = c_{TMD} / c_{str} \tag{3}$$

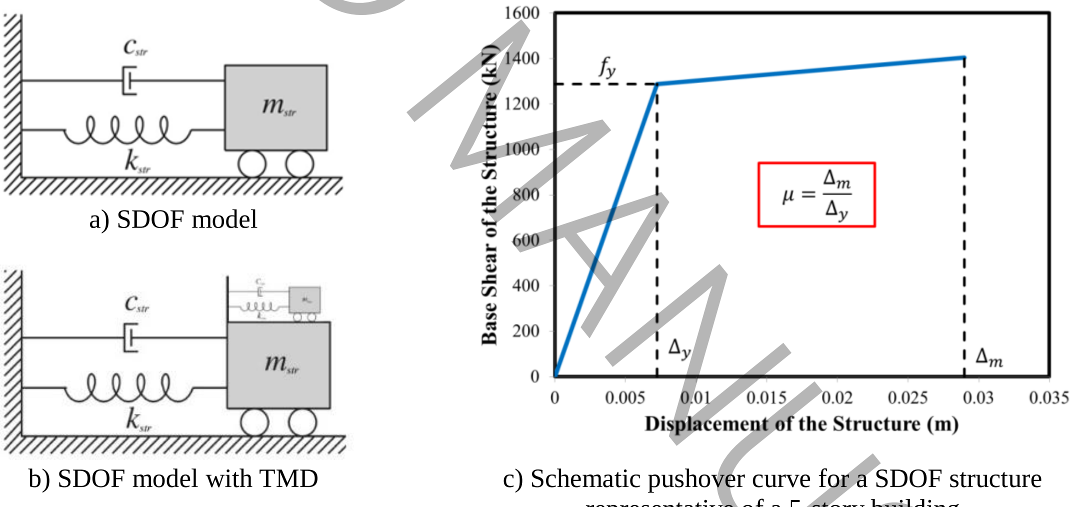


Fig. 1. Schematic diagram of SDOF models and structural behavior curve

To conduct numerical analyses, two values of 0.05 and 0.1 are considered for $m_r$. Since it is assumed that $m_r = c_r$, the same values apply to $c_r$. It should be noted that the damping ratio for the structure is taken as 5%. The aim of this study is to assess the influence of TMD stiffness variation on the structural response. Therefore, the stiffness ratio $k_r$ varies from 0.01 to 0.5. In this research, it is assumed that the structure behaves both elastically and inelastically. For inelastic structures, a bilinear hysteretic model is adopted. In Fig. 1(c), the schematic pushover curve for a SDOF structure representative of a 5-story building is illustrated. The yield strength for the systems is determined based on Standard 2800 seismic code [34]. The ductility ($\mu$) of structure is introduced in Equation 4.

$$\mu = \left(\Delta_m / \Delta_y\right)_{str} \tag{4}$$

In Equation 4, $\Delta_m$ and $\Delta_y$ are the maximum and yielding displacements of the structure, respectively. Two ductility levels of 1 and 4 are considered in this study. For a traditional TMD, the properties are adjusted to match the dynamic characteristics of the structure's fundamental mode. Therefore, the parameters are assumed to be $m_r = k_r = c_r$ in a traditional TMD. In the current study, 20 ground motions recorded on site class C were selected. The ground motion characteristics are summarized in Table 1. The ground motion suite was selected in accordance with FEMA-440 [35], and the records were obtained from the PEER Ground Motion Database [36].

Table 1. Properties of the selected ground motion records, obtained from the PEER Ground Motion Database [36] and summarized according to FEMA-440 [35].

| Number | Date | Earthquake Name | Magnitude (Ms) | Station Name | Station Number | Component (deg) | PGA (cm/s2) |
|---|---|---|---|---|---|---|---|
| 1 | 10/15/1979 | Imperial Valley | 6.8 | El Centro, Parachute Test Facility | 5051 | 315 | 200.2 |
| 2 | 2/9/1971 | San Fernando | 6.5 | Pasadena, CIT Athenaeum | 80053 | 90 | 107.9 |
| 3 | 2/9/1971 | San Fernando | 6.5 | Pearblossom Pump | 269 | 21 | 133.4 |
| 4 | 6/28/1992 | Landers | 7.5 | Yermo, Fire Station | 12149 | 0 | 167.8 |
| 5 | 10/17/1989 | Loma Prieta | 7.1 | APEEL 7, Pulgas | 58378 | 0 | 153 |
| 6 | 10/17/1989 | Loma Prieta | 7.1 | Gilroy #6, San Ysidro Microwave site | 57383 | 90 | 166.9 |
| 7 | 10/17/1989 | Loma Prieta | 7.1 | Saratoga, Aloha Ave. | 58065 | 0 | 494.5 |
| 8 | 10/17/1989 | Loma Prieta | 7.1 | Gilroy, Gavilon College Phys Sch Bldg | 47006 | 67 | 349.1 |
| 9 | 10/17/1989 | Loma Prieta | 7.1 | Santa Cruz, University of California | 58135 | 360 | 433.1 |
| 10 | 10/17/1989 | Loma Prieta | 7.1 | San Francisco, Diamond Heights | 58130 | 90 | 110.8 |
| 11 | 10/17/1989 | Loma Prieta | 7.1 | Fremont, Mission San Jose | 57064 | 0 | 121.6 |
| 12 | 10/17/1989 | Loma Prieta | 7.1 | Monterey, City Hall | 47377 | 0 | 71.6 |
| 13 | 10/17/1989 | Loma Prieta | 7.1 | Yerba Buena Island | 58163 | 90 | 66.7 |
| 14 | 10/17/1989 | Loma Prieta | 7.1 | Anderson Dam, Downstream | 1652 | 270 | 239.4 |
| 15 | 4/24/1984 | Morgan Hill | 6.1 | Gilroy, Gavilon College Phys Sci Bldg | 47006 | 67 | 95 |
| 16 | 4/24/1984 | Morgan Hill | 6.1 | Gilroy #6, San Ysidro Microwave Site | 57383 | 90 | 280.4 |
| 17 | 7/8/1986 | Palmsprings | 6 | Fun Valley | 5069 | 45 | 129 |
| 18 | 1/17/1994 | Northridge | 6.8 | Littlerock, Brainard Canyon | 23595 | 90 | 70.6 |
| 19 | 1/17/1994 | Northridge | 6.8 | Castaic, Old Ridge Route | 24278 | 360 | 504.2 |
| 20 | 1/17/1994 | Northridge | 6.8 | Lake Hughes #1, Fire station #78 | 24271 | 0 | 84.9 |

## 3. Assessment of the response of SDOF systems under earthquake records

In the following, the effect of the TMD mass on the structural response is examined under 20 real earthquake records. The responses of two structures with periods of 0.5 and 1 second are analyzed, considering ductility levels of $\mu$ =1 and 4. The ductility is defined as the ratio of maximum displacement of the systems to the yield displacement. In the studied structures, it is assumed that $m_r = c_r$. In Fig. 2, the average response ratio ($D_r$) for the structure with a period of 0.5 seconds under 20 ground motions is evaluated. $D_r$ is defined as the ratio of the maximum response of the structure with TMD, $(\Delta_{\max})_{With-TMD}$, to its corresponding maximum response without installing TMD, $(\Delta_{\max})_{Without-TMD}$, under earthquake excitation, as expressed in Equation 5:

$$D_r = \frac{(\Delta_{\max})_{with\ TMD}}{(\Delta_{\max})_{without\ TMD}} \tag{5}$$

Comparing Figs. 2(a) and 2(c) shows that increasing the mass ratio results in a slight decrease in $D_r$ when the models behave elastically. However, a slight increase in the inelastic state can be observed by comparing Figs. 2(b) and 2(d). Generally, increasing the mass ratio from 0.05 to 0.1 has little effect on $D_r$ of the studied models.

It is observed that when using a traditional TMD with parameters $m_r = k_r = c_r = 0.1$, the value of $D_r$ at a ductility level of 1 is 0.96. In other words, the structural response is reduced by only 4% on average. However, by reducing $k_r$ from 0.1 to 0.05, $D_r$ can be reduced to a minimum value of 0.86 on average. In Fig. 2(d), it is shown that increasing the ductility level to 4 results in $D_r$ reaching 1.07 when using a traditional TMD. In other words, the presence of the TMD leads to an increase in the structural response under nonlinear behavior. However, when $k_r$ is reduced to 0.05, a minimum $D_r$ of 1.02 can be achieved on average. Despite this decrease, the value remains greater than 1, indicating that the TMD does not contribute to reducing the structural response on average.

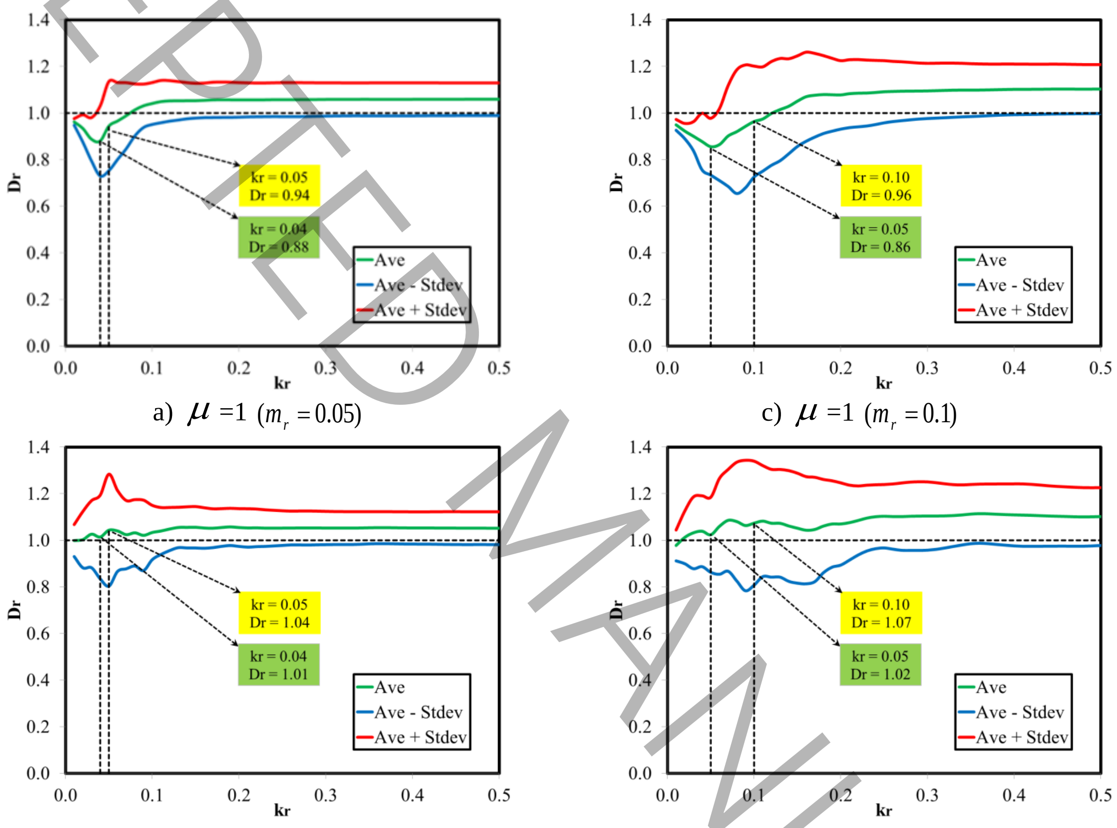


a) $\mu = 1$ $(m_r = 0.05)$ c) $\mu = 1$ $(m_r = 0.1)$

b) $\mu = 4$ $(m_r = 0.05)$ d) $\mu = 4$ $(m_r = 0.1)$

Fig. 2. Effect of stiffness variations on $D_r$ under 20 ground motions for a structure with period of 0.5 s.

In Fig. 3(a), $D_r$ for a structure with a period of 1 second is illustrated. It is observed that when using a traditional TMD with $m_r = k_r = c_r = 0.1$, the value of $D_r$ at a ductility of 1 is 0.82. By reducing $k_r$ from 0.1 to 0.07, a minimum $D_r$ of 0.76 can be achieved on average. In Fig. 3(b), it is observed that for a system with ductility level of 4, the value of $D_r$ equals 1.07 when using a traditional TMD. In other words, the presence of the tuned mass damper leads to an increase in the structural response under nonlinear behavior. By reducing $k_r$ to 0.05, a minimum $D_r$ of 0.91 can be achieved on average. However, as demonstrated in Fig. 3(c), increasing the ductility level to 6 can lead to a reduction in the effectiveness of the TMD. As anticipated, comparing the results in Figs. 2 and 3 shows that TMD effectiveness strongly depends on the frequency content and predominant periods of the ground motions relative to the structural period. Comparing Figs. 2(c) and 2(d) with Figs. 3(a) and 3(b) respectively, shows that the TMD is more effective for the structure with a 1-second period than for the one with a 0.5-second period.

The improved performance of the TMD with reduced stiffness in nonlinear structures can be explained through the concept of period elongation. When a structure yields during strong seismic excitation, its effective natural period lengthens [35]. A traditional TMD, tuned to the elastic fundamental frequency of the structure, becomes detuned under these conditions, and its effectiveness either diminishes or may even amplify the response. Reducing the TMD stiffness while keeping the TMD mass constant lowers its natural frequency, bringing it closer to the elongated period of the yielded structure and thereby restoring the tuning condition.

For a given ductility, the absolute elongation of the effective period of a yielded structure is proportional to its initial period [35]. Thus, a 0.5 s structure undergoes a smaller absolute period shift than a 1.0 s structure, so a traditional TMD remains less severely detuned, and the additional benefit of reducing TMD stiffness is inherently smaller. Moreover, the slight period shift caused by the added TMD mass can noticeably affect $D_r$ of short-period systems, because their response is highly sensitive to small period changes while the reference uncontrolled displacement used in $D_r$ remains fixed. The combination of these two effects explains the smaller improvement from stiffness reduction observed for the 0.5 s structure compared to the 1.0 s structure, as seen in Figs. 2 and 3.

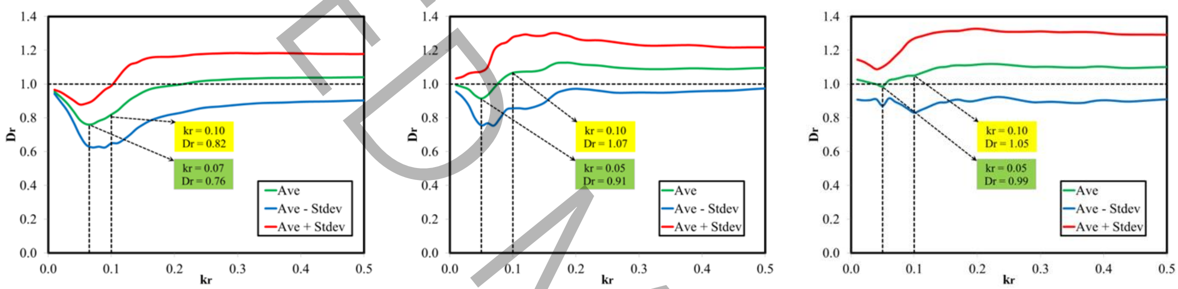


a) $\mu$ =1 b) $\mu$ =4 c) $\mu$ =6

Fig. 3. Effect of stiffness variations on $D_r$ under 20 records for a structure with 1 second period.

### 3.1. Comparison of Results with Previous Studies

Figs. 4(a) and 4(b) present the optimum TMD periods corresponding to the minimum $D_r$ for both structures with periods of 0.5 s and 1 s, and for two ductility levels: 1 (thick blue line) and 4 (dashed blue line), under each ground motion. The red lines indicate the TMD periods proposed in the current study, which correspond to the minimum $D_r$ obtained from Figs. 2 and 3. The green lines represent the traditional TMD period, which is tuned to the fundamental period of each structure. Considering the mass ($m_{TMD}$) and the stiffness ($k_{TMD}$) of TMD, its period is determined using the following equation:

$$T_{TMD} = 2\pi\sqrt{m_{TMD} / k_{TMD}} \tag{6}$$

It can be seen that the proposed periods in the current study for different structures are greater than the traditional periods of TMDs. Moreover, in most cases, the optimum TMD period increases as the ductility level increases. In Figs. 4(c) and 4(d), the distributions of $D_r$ corresponding to different TMD periods are presented. In these graphs, the vertical axis represents the percentage of $D_r$ values that are smaller than a specific value. It can be seen that for both structures, using the optimum TMD leads to a reduction in the structural response for all elastic cases. Since the properties of the optimum TMD vary for each ground motion, this approach is impractical for passive systems, and a tunable mechanism would be required. If the TMD proposed in the current study is used, then in 95% of cases, the TMD reduces the response of the structure. Furthermore, for both structures, the effectiveness of the proposed TMD is superior to that of the traditional TMD. At higher ductility levels, the optimum TMD reduces the structural response in 95% and 85% of cases for the 5-story and 10-story structures, respectively. The performance of the proposed TMD is considerably better than that of the traditional TMD; however, its effectiveness in reducing the structural response declines to 40% and 70% for the 5-story and 10-story structures, respectively. In general, it can be concluded that adopting a lower TMD stiffness compared to the traditional value can improve the effectiveness of the TMD in reducing the structural response for both elastic and inelastic conditions.

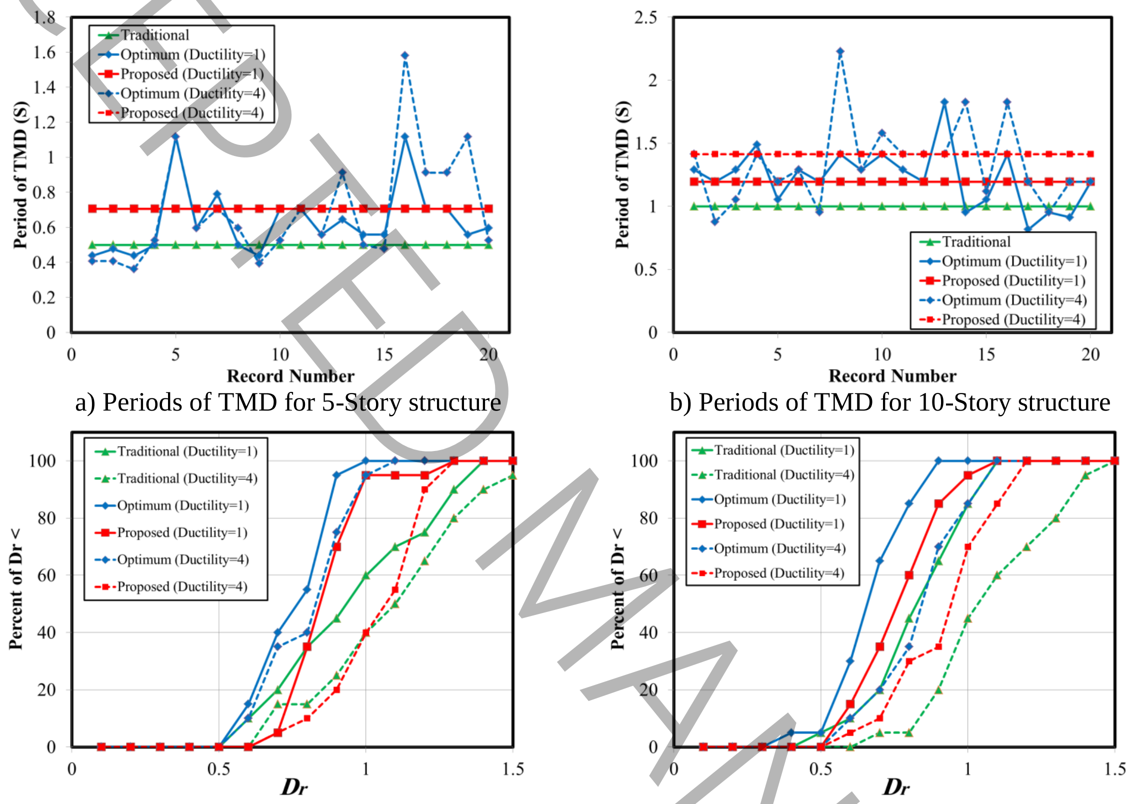


a) Periods of TMD for 5-Story structure

b) Periods of TMD for 10-Story structure

c) Percentage of $D_r$ smaller than a specific value for 5-story structure

d) Percentage of $D_r$ smaller than a specific value for 10-story structure

Fig. 4. Traditional, optimum, and proposed TMD periods, and distributions of $D_r$ corresponding to different TMD periods.

For comparison with previous findings, several classical optimization formulas are selected from the studies of Den Hartog [2], Sadek et al. [4], Warburton [5], and Leung and Zhang [6]. In these studies, the optimized parameters of the TMD system are calculated based on the first mode of vibration of the structure. In these formulas, the mass ratio $m_r$ is represented by the symbol $\mu$, and the optimum frequency ratio $f_{opt}$ is defined as the ratio of the optimally tuned TMD frequency to the fundamental frequency of the structure. The optimum damping ratio of the TMD is represented by $\xi_{opt}$. The following equations illustrate the relationship between the mentioned parameters and those used in the present study.

$$f_{opt} = \frac{(\omega_{TMD})_{opt}}{\omega_{STR}} = \frac{\sqrt{((k_r)_{opt} \times k_{str}) / (m_r \times m_{str})}}{\sqrt{k_{str} / m_{str}}} = \sqrt{\frac{(k_r)_{opt}}{m_r}} \tag{7}$$

$$\xi_{opt} = \frac{c_{TMD}}{2m_{TMD}\left(\omega_{TMD}\right)_{opt}} = \frac{c_r \times c_{STR}}{2m_r \times m_{STR}\sqrt{\frac{\left(k_r\right)_{opt} \times k_{STR}}{m_r \times m_{STR}}}} = \sqrt{\frac{m_r}{\left(k_r\right)_{opt}}}\xi_{str} \tag{8}$$

In the above equations, the parameter $(k_r)_{opt}$ represents the optimum stiffness ratio obtained in the current study, and $\xi_{str}$ represents the damping ratio of the structure. Equation 8 provides the complete relationship between the optimal TMD damping ratio known from classical formulations and the dimensionless damping coefficient ratio ($c_r$) adopted in the current study, assuming that $c_r = m_r$.

In Table 2, the properties of the optimal TMD proposed in the current study are compared with the findings of previous studies. It should be noted that the present study does not investigate the influence of damping variations and focuses solely on stiffness coefficient variations. Moreover, the equations provided in the reviewed studies for calculating optimal TMD properties do not incorporate any provisions for nonlinear structures; therefore, the same characteristics were also applied to the nonlinear case. An examination of the frequency ratio indicates that the optimal frequency ratio obtained in the present study is somewhat lower than those recommended by previous studies.

Table 2. Comparison of the proposed optimum TMD with TMDs from previous studies: properties and performance.

| $T_{str}$ | $m_r$ | $\mu$ | $f_{opt}(\xi_{opt}\%)$ | | | | | $(D_r)_{PS}$ | $(D_r)_{CS}$ |
|---|---|---|---|---|---|---|---|---|---|
| | | | Current Study | Den Hartog [2] | Sadek et al. [4] | Warburton [5] | Leung and Zhang [6] | | |
| 0.5 | 0.05 | 1 | 0.894 (5.6%) | 0.95 (13%) | 0.94 (26%) | 0.94 (11%) | 0.91 (11%) | 0.87 | 0.88 |
| 0.5 | 0.05 | 4 | 0.894 (5.6%) | | | | | 1.03 | 1.01 |
| 0.5 | 0.1 | 1 | 0.707 (7.1%) | 0.91 (18%) | 0.90 (35%) | 0.89 (15%) | 0.85 (15%) | 0.84 | 0.86 |
| 0.5 | 0.1 | 4 | 0.707 (7.1%) | | | | | 1.05 | 1.02 |
| 1.0 | 0.1 | 1 | 0.837 (6%) | 0.91 (18%) | 0.90 (35%) | 0.89 (15%) | 0.85 (15%) | 0.8 | 0.76 |
| 1.0 | 0.1 | 4 | 0.707 (7.1%) | | | | | 1.01 | 0.91 |

In the next step, based on previous studies, an average value for the optimal frequency ratio and damping ratio was calculated for each system. The optimal system derived from previous studies was then subjected to the suite of earthquake ground motion records considered in this research. Table 2 presents the average displacement reduction ratio for this system, denoted as $(D_r)_{PS}$, along with the corresponding values obtained in the current study for the proposed systems, denoted as $(D_r)_{CS}$. It can be concluded that the seismic performance of the proposed TMD is comparable to, and acceptable relative to, the classically optimized TMD. Notably, under conditions of structural nonlinearity, the proposed TMD demonstrates superior performance compared to the classically optimized TMD.

### 3.2. Effect of using partial structural mass as a TMD on SDOF system response

One of the issues with a TMD is the significant additional mass placed on the top floor of the structure, which can lead to an increase in the cross-sections of structural load-bearing elements and higher construction costs. Moreover, as shown in Fig. 2, increasing the mass of the TMD may enhance its effectiveness in reducing the structural response in some cases. However, due to design considerations and construction costs, the effectiveness of the TMD is limited by the constraints on its mass.

In this section, the idea of utilizing a portion of the building's mass, such as the roof floor, as a Tuned Structural Mass Damper (TSMD) [26] is considered. The TSMD concept can be physically realized by isolating a portion of the roof mass using seismic isolators, which allow relative motion between the TSMD mass and the primary structure [27]. Then, similar to the previous section, the stiffness of the TSMD is varied in order to optimize its performance. The schematic structure of this type of TMD is illustrated in Fig. 5. It is evident that avoiding an increase in the total mass of the structure will likely lead to a reduction in the cross-sections of load-bearing elements. The implications of this approach on the seismic response of the structure are further explored.

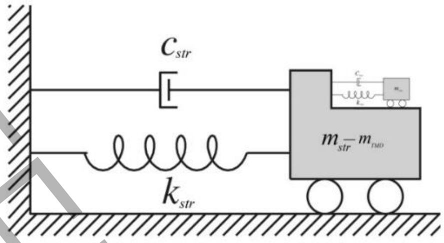


Fig.5. SDOF systems with TSMD

Fig. 6 compares the average $D_r$ between two scenarios: one in which the TMD mass is added to the system (gray line) and another in which a portion of the structural mass serves as the TMD mass (green line). For both ductility levels of 1 and 4, using a part of the structural mass as the TMD mass reduces $D_r$ for both 0.5 s and 1 s structures. Overall, the results demonstrate that the effectiveness of the TSMD is superior to that of both the traditional TMD and the TMD proposed in the previous section.

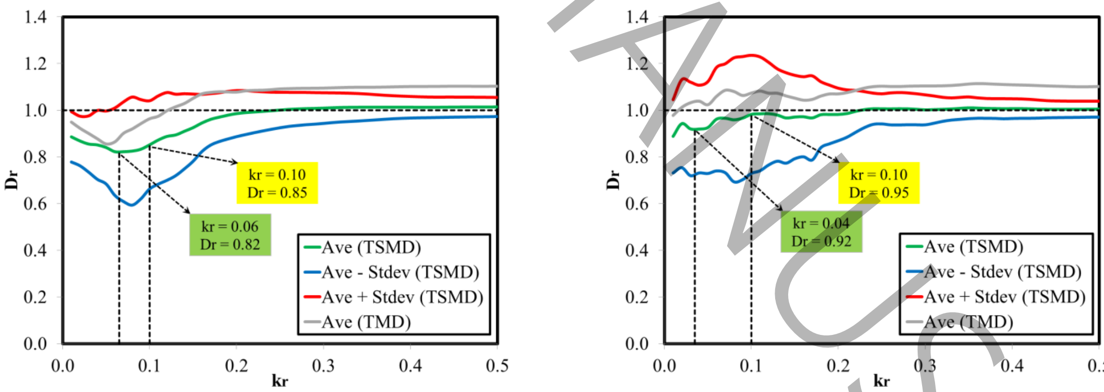


a) Equivalent SDOF model of a 5-story building ( $\mu$ =1 )

b) Equivalent SDOF model of a 5-story building ( $\mu$ =4 )

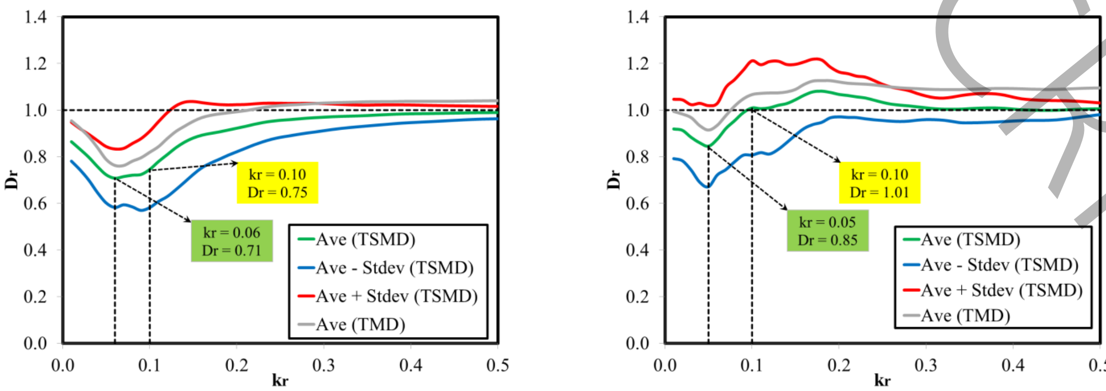

c) Equivalent SDOF model of a 10-story building ($\mu$ =1 )

d) Equivalent SDOF model of a 10-story building ($\mu$ =4 )

Fig. 6. Comparison of the effectiveness of the TSMD, traditional TMD, and proposed TMD under varying $k_r$

**4. Assessment of the response of MDOF systems under earthquake records**

In this section, a 10-story shear building model is assessed as illustrated in Fig. 7(a). The fundamental vibration period of the first mode of the model is assumed to be $T_{str} = 1s$ . The structure was evaluated in both elastic and inelastic states. For the nonlinear analyses, the structure was designed according to Standard 2800 [34], with a bilinear hysteretic model considered for each floor.

The structure was subjected to 20 earthquake records, and the maximum story displacements and relative inter-story drifts were calculated. The responses of the structure were assessed for three cases:

1- In the first case, as shown in Fig. 7(a), the structure is subjected to ground motions without a TMD.

2- In the second case, as shown in Fig. 7(b), a TMD is placed on the tenth floor, and by varying the TMD stiffness, the responses of the floors under each earthquake record are compared with their corresponding values in the first case (system without TMD) to determine the TMD properties that yield the best performance. The placement of the TMD at the top floor is the most common and widely recommended configuration in both research and practice, as it corresponds to the location of maximum modal displacement for the fundamental mode, where the TMD is most effective. Studies have shown that positioning TMDs within the upper one-third of the structure yields the most pronounced improvements in response reduction [37].

3- In the third case, as shown in Fig. 7(c), a portion of the tenth floor's mass is considered as the TMD mass, and by varying the TMD stiffness, the responses of the floors under each earthquake record are compared to their corresponding values in the first case (system without TMD) to determine the TMD properties that yield the best performance.

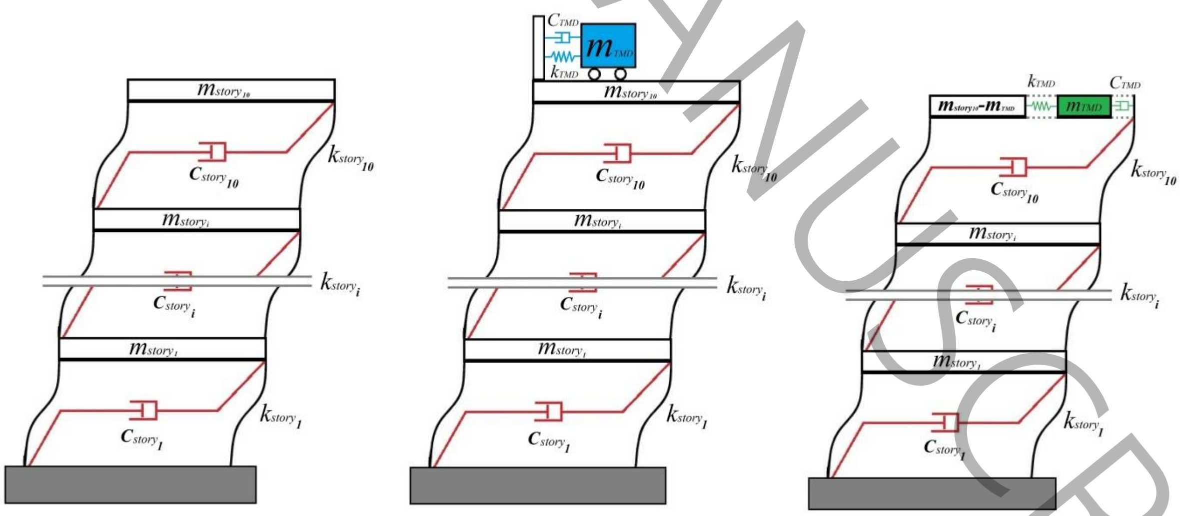


a) Structure without TMD

b) Structure with TMD

b) Structure with TSMD

Fig. 7. 10-story building models

In the analyses, the mass $(m_{story})$, stiffness $(k_{story})$, and damping $(c_{story})$ of all stories are considered identical. The TMD properties are determined based on the mass ratio $(m_{rs})$, the TMD to story stiffness ratio $(k_{rs})$, and damping coefficient ratio $(c_{rs})$ presented in Equations 9 to 11.

$$m_{TMD} = m_{rs} \times m_{story} \tag{9}$$

$$k_{TMD} = k_{rs} \times k_{story} \tag{10}$$

$$c_{TMD} = c_{rs} \times c_{story} \tag{11}$$

Fig. 8 presents the maximum story displacement ratio $(D_r)_i$ and the maximum inter-story drift ratio $(DR_r)_i$. The ratios are calculated using Equations 12 and 13.

$$(D_r)_i = \left( \frac{(\Delta_{\max})_{with\ TMD}}{(\Delta_{\max})_{without\ TMD}} \right)_{i^{th} Story} \tag{12}$$

$$(DR_r)_i = \left( \frac{(Drift_{\max})_{with\ TMD}}{(Drift_{\max})_{without\ TMD}} \right)_{i^{th} Story} \tag{13}$$

In the above equations, $(\Delta_{\max})_{With-TMD}$ and $(\Delta_{\max})_{Without-TMD}$ denote the maximum story displacement with and without TMD, respectively, while $(Drift_{\max})_{With-TMD}$ and $(Drift_{\max})_{Without-TMD}$ are the maximum story drift with and without TMD, respectively. For the analyses performed in this section, the TMD mass is considered to be 50% of the tenth floor's mass, or, in the other words, 5% of the total mass of the structure, which is a practical value in constructed buildings. The corresponding stiffness ratio $k_{rs}$ for a traditional TMD was determined based on the floor masses and story stiffnesses of the 10-story building. The calculation assumed that the TMD period was matched to the structure's fundamental period of 1 second. Consequently, the ratio of the TMD's stiffness to the building's story stiffness was found to be $k_{rs} = k_{TMD} / k_{story} = 0.0114$ .

**4.1. Seismic response assessment of the 10-story model equipped with TMD**

In Fig. 8(a), the displacement ratio $(D_r)_i$ for the elastic structure is presented. The results indicate the traditional TMD with $k_{rs} = 0.0114$ reduces the displacement of the first floor by 21% $((D_r)_1 = 0.79)$, and that of the tenth floor by approximately 20% $((D_r)_{10} = 0.80)$. As shown in Fig. 8(b), a traditional TMD with $k_{rs} = 0.0114$ leads to an increase in the drift ratio $(DR_r)_i$ from lower to upper stories, and the drift ratio at the tenth story $(DR_r)_{10}$ exceeds 1, indicating that its effectiveness in mitigating drift diminishes at higher floors and that the drift of the tenth story actually increases when a traditional TMD is installed. The results for the inelastic structure in Fig. 8(c) show that the traditional TMD with $k_{rs} = 0.0114$ reduces the displacement of the first floor by 8% $((D_r)_1 = 0.92)$, while the tenth-floor displacement is reduced by only about 1.4% $((D_r)_{10} = 0.986)$. In Fig. 8(d), the drifts of 8$^{th}$, 9$^{th}$, and 10$^{th}$ stories increase significantly due to the installation of the TMD. Fig. 8(c) also shows that increasing the $k_{rs}$ to 0.0142 reduces the displacements of the first to fourth floors, whereas the displacement ratios ($(D_r)_i$) increase in the other stories. A comparison of different subfigures in Fig. 8 indicates that the effectiveness of the traditional TMD significantly deteriorates when the structure exhibits inelastic behavior.

In Fig. 8, it can be observed that for the lower stories of the elastic structure, the minimum values of $(D_r)_i$ and $(DR_r)_i$ are found when $k_{rs} = 0.0114$, which corresponds to the traditional value. As the floor level increases, the minimum values of $(D_r)_i$ and $(DR_r)_i$ for the upper stories are observed at $k_{rs} < 0.0114$. Additionally, as demonstrated in Fig. 8, for the lower stories of the inelastic structure, the minimum values of $(D_r)_i$ and $(DR_r)_i$ are associated with $k_{rs} > 0.0114$. As the floor increases further, the minimum values of $(D_r)_i$ and $(DR_r)_i$ for the upper stories are observed at $k_{rs} < 0.0114$.

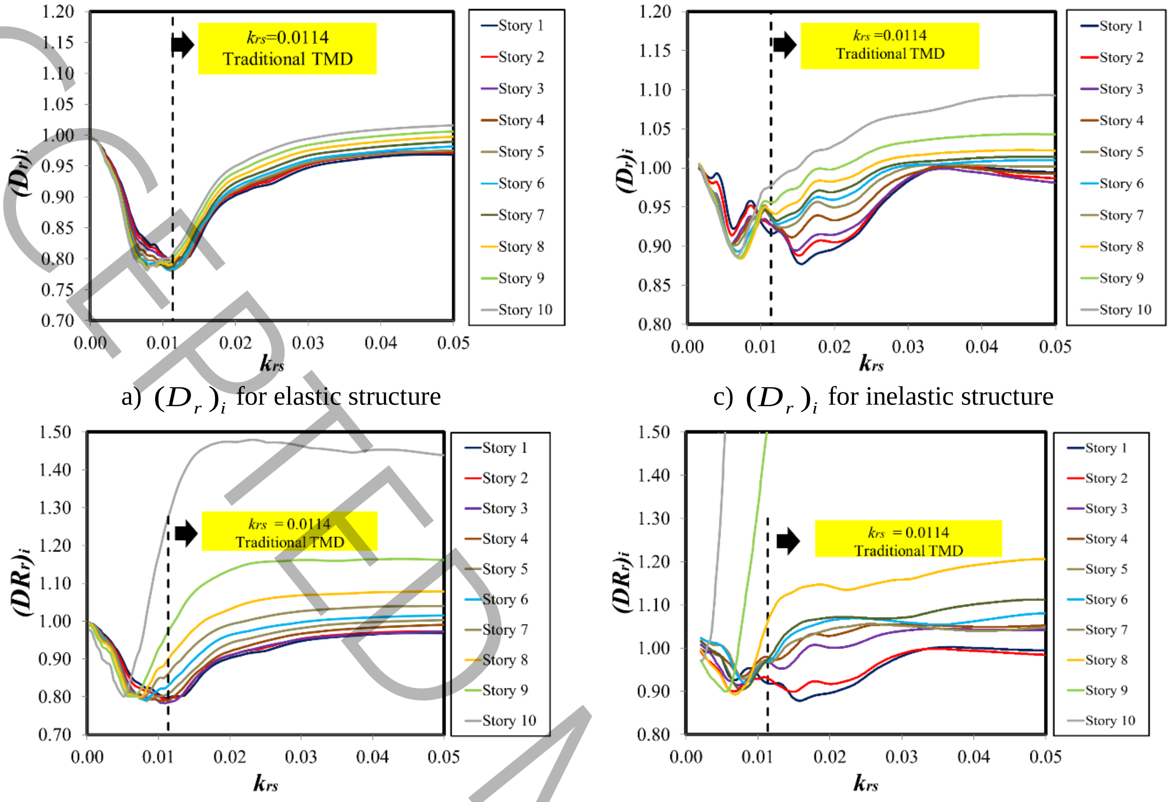


a) $(D_r)_i$ for elastic structure

c) $(D_r)_i$ for inelastic structure

b) $(DR_r)_i$ for elastic structure

d) $(DR_r)_i$ for inelastic structure

Fig. 8. Effects of varying $k_{rs}$ of TMD on the response of 10-story model under 20 ground motions $(m_{rs} = 0.5)$

In Fig. 9(a), the average ratios of $(D_r)_i$ and $(DR_r)_i$ for all 10 stories are plotted versus variations of $k_{rs}$ for the elastic structure. Investigating the structural response at the two $k_{rs}$ values corresponding to the two identified minima in Fig. 9(a) is of particular importance. The first minimum occurs at $(k_{rs})_{Min1} = 0.0053$, which is less than the value corresponding to the traditional TMD, while the second minimum occurs at $(k_{rs})_{Min2} = 0.0138$, which is greater than the value corresponding to the traditional TMD. As observed in Fig. 9(b), using TMD1, which employs a stiffness lower than that of the traditional TMD, results in a greater reduction in the displacement of all stories; however, this reduction is more significant in the upper stories. In the lower stories, the effectiveness of TMD1 is reduced compared to that of the traditional TMD.

On the other hand, using TMD2, which employs a stiffness value higher than that of the traditional TMD, leads to a greater reduction in the displacement of stories 6 and above compared to the traditional TMD. However, the effectiveness of TMD2 is similar to that of traditional TMD for the lower stories. Fig. 9(c) demonstrates that the $(DR_r)_i$ values corresponding to TMD1 are significantly smaller than those corresponding to both TMD2 and the traditional TMD for stories 5 and above. Although $(DR_r)_i$ values corresponding to TMD1 are greater than their corresponding values for TMD2 and the traditional TMD in the lower stories, the increase in $(DR_r)_i$ is less than 4% and its maximum value for the first story is 0.84.

In Fig. 9(d), both $k_{rs}$ values corresponding to the minimum $(D_r)_i$ and $(DR_r)_i$ are smaller than the traditional $k_{rs}$ for the inelastic structure. Figs. 9(e) and (f) demonstrate that the effectiveness of TMD3 is significantly better than that of TMD4 and that of the traditional TMD. It should be noted that the traditional TMD increases the drift of stories 8 to 10.

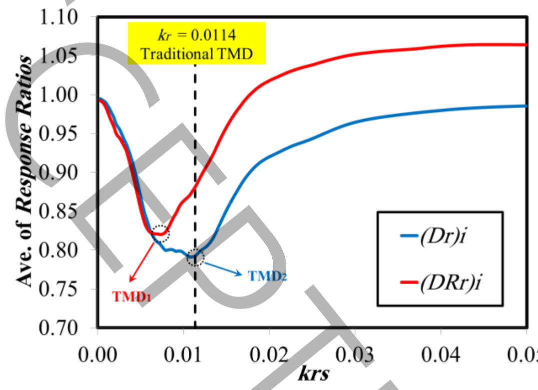


a) Average of $(D_r)_i$ and $(DR_r)_i$ for all stories (Elastic structure)

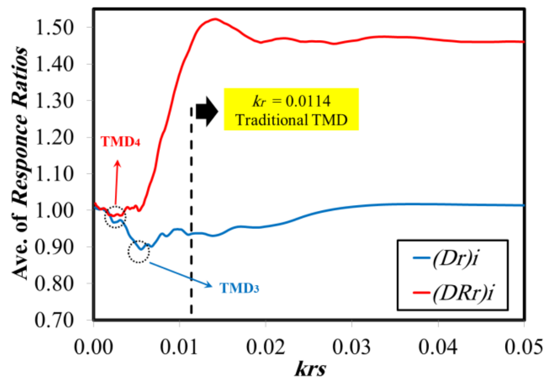


d) Average of $(D_r)_i$ and $(DR_r)_i$ for all stories (Inelastic structure)

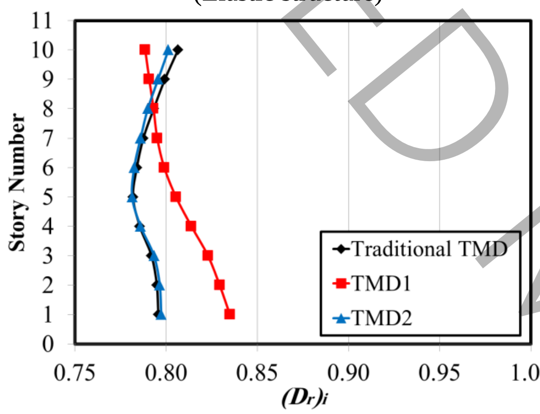


b) Distribution of minimum $(D_r)_i$ over stories (Elastic structure)

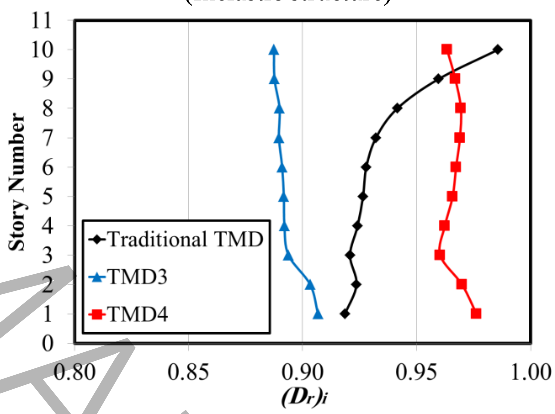


e) Distribution of minimum $(D_r)_i$ over stories (Inelastic structure)

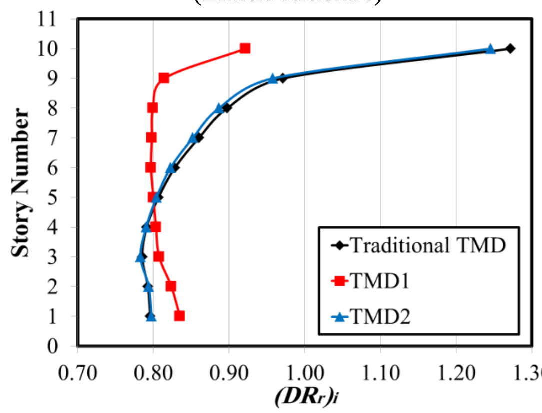


c) Distribution of minimum $(DR_r)_i$ over stories (Elastic structure)

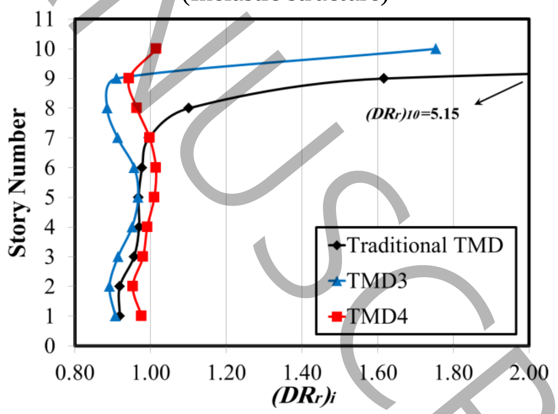


f) Distribution of $(DR_r)_i$ over stories (Inelastic structure)

Fig. 9. Comparison of different optimum $k_{rs}$ values on $(D_r)_i$ and $(DR_r)_i$

In Table 3, the values of $k_{rs}$ corresponding to the minimum $(D_r)_i$ and $(DR_r)_i$ are presented. It can be observed that reducing the stiffness of TMD relative to the traditional value enhances the effectiveness of the TMD in both elastic and inelastic structures. $k_{rs}$

Table 3. The values of $k_{rs}$ corresponding to the minimum $(D_r)_i$ and $(DR_r)_i$

| | $TMD_T$ | $TMD_1$ | $TMD_2$ | $TMD_3$ | $TMD_4$ |
|---|---|---|---|---|---|
| $k_{rs}$ | 0.0114 | 0.0073 | 0.0109 | 0.0055 | 0.0023 |

**4.2. Seismic response assessment of the 10-story model equipped with TSMD**

In the subsequent phase of this study, the idea of using the structural mass as the TMD mass (TSMD) is investigated for a 10-story structure. In this study, 50% of the 10th floor mass was considered as the TSMD mass $(m_{rs} = 0.5)$. In other words, the mass of the TMD was assumed to be 5% of the total mass of the structure. The TSMD mass was then connected to the 10th floor, and the structural response was evaluated under 20 recorded ground motions by varying the stiffness of the TSMD.

As shown in Fig. 10, the use of the TSMD leads to a reduction in the $(D_r)_i$ ratio for the 7th and 10th floors. However, for the 1st and 4th floors, when $k_{rs}$ is less than the traditional stiffness ratio, no significant change in the $(D_r)_i$ ratio is observed. When $k_{rs}$ exceeds the traditional value, the use of the TSMD results in an increase in the $(D_r)_i$ ratio. Nevertheless, the $(D_r)_i$ ratio remains below unity for the 1st and 4th floors, indicating that the structural response is still reduced. Moreover, unlike traditional TMDs, this approach does not impose any additional mass on the structure.

According to Fig. 11, the use of the TSMD can decrease $(DR_r)_i$ ratio of the 1st, 4th, 7th, and 10th stories when $k_{rs}$ equals to the traditional stiffness ratio and its effects on the 7th and 10th story are significant. If $k_{rs}$ is decreased, then the effectiveness of the TSMD improves significantly, especially for the upper stories.

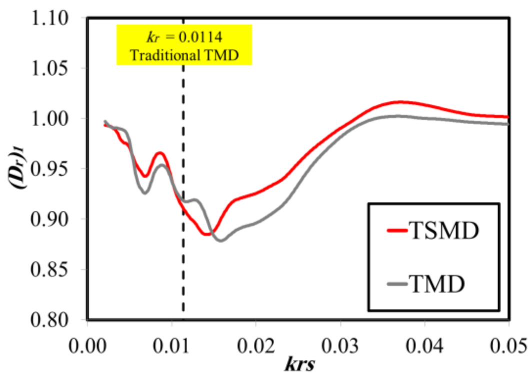

a) 1st story

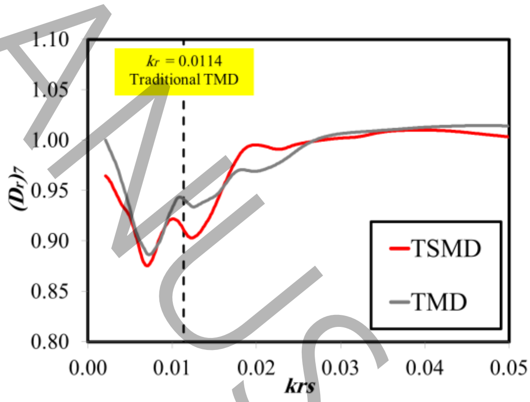

c) 7th story

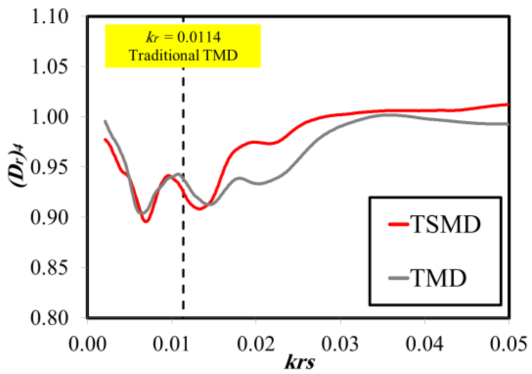

b) 4th story

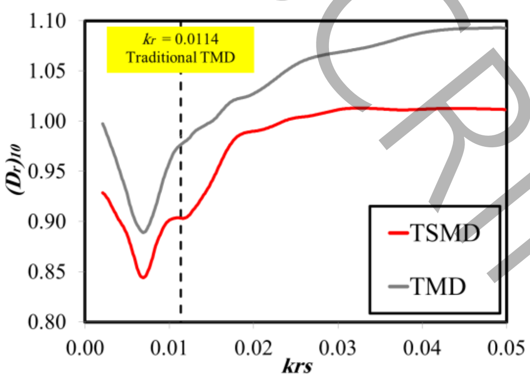

d) 10th story

Fig. 10. Average of $(D_r)_i$ for floors 1, 4, 7, and 10 under 20 records in the cases of using TMD and TSMD

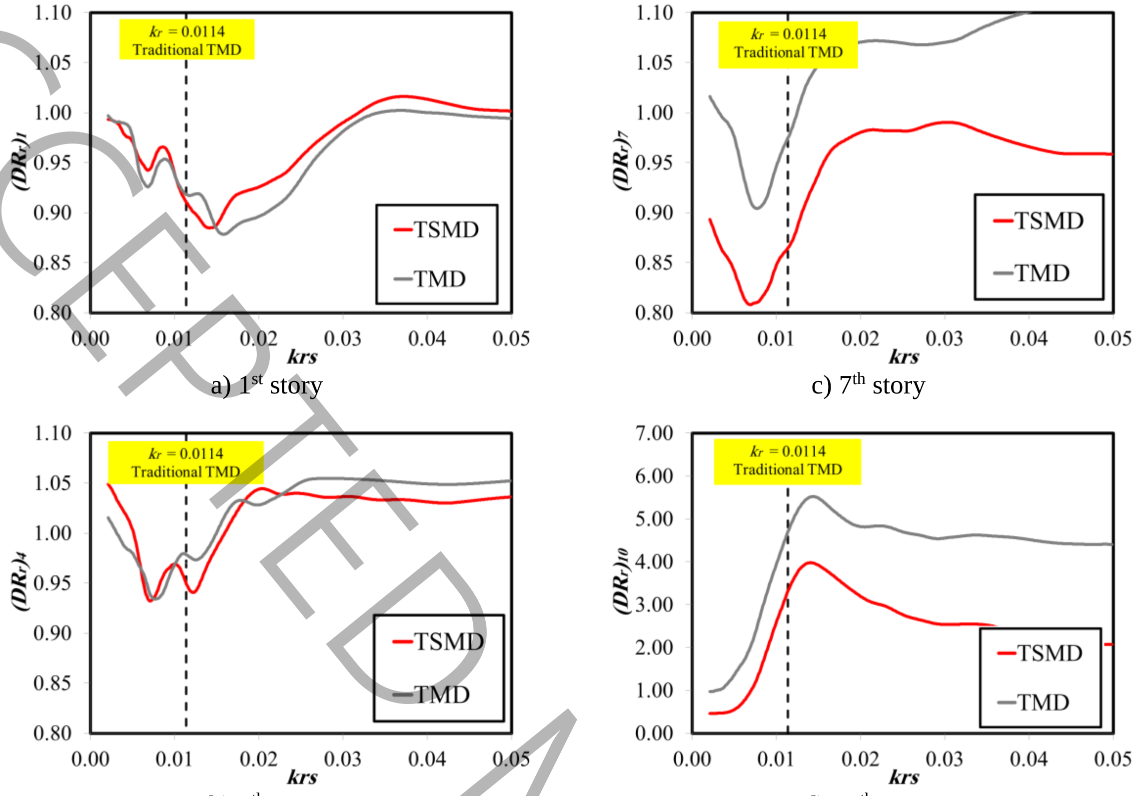


a) 1st story

c) 7th story

b) 4th story

d) 10th story

Fig.11. The average of $(DR_r)_i$ for floors 1, 4, 7, and 10 under 20 records in the cases of using TMD and TSMD

## 5. Conclusions

### 5.1. Summary of Findings

A comprehensive parametric investigation of Tuned Mass Dampers (TMDs) was performed to assess their effectiveness in mitigating the seismic response of structures. For this purpose, several SDOF and MDOF systems were analyzed under a set of ground motions. The systems were evaluated considering both linear and nonlinear behavior. The study focused on identifying the optimal TMD stiffness for minimizing structural seismic response, and on proposing a novel TMD configuration. The main results of the study are as follows:

- For SDOF structures, the study demonstrated that traditional TMDs with standard parameters (for instance, $m_r = k_r = c_r = 0.1$) provide only modest response reduction in elastic structures, achieving reductions of just 4% and 18% for structures with periods of 0.5 s and 1 s, respectively, under the excitations studied in the current research.

- More significantly, the research revealed that in nonlinear systems at a ductility level of 4, traditional TMD configurations can increase the structural response by up to 7%, highlighting a fundamental limitation of traditional approaches.

- Parametric analyses showed that reducing $k_r$ below the traditional value improves the performance of the TMD. The optimal $k_r = 0.05$ for a structure with a period of 0.5 s and $k_r = 0.07$ for a structure with a period of 1 sec were determined based on minimizing displacement ratios under the excitations. The response ratios ( $D_r$ ) decreased to 0.86 and 0.76 for the elastic structures with periods of 0.5 s and 1 s, respectively. Also, the results showed that the optimal $k_r = 0.05$ for both the 0.5s and 1s structures improves the effectiveness of TMD in a nonlinear structure. It should be noted that the value of the optimal $k_r$ is smaller than the traditional value for both elastic and inelastic systems.

- For the 10-story MDOF building model, the study identified two optimal TMD-to-story stiffness ratios ($k_{rs}$) based on the minima of the average of drift ratio $(DR_r)_i$ and the average displacement ratio $(D_r)_i$ for all stories. It was observed that the optimal TMD associated with the minimum average $(DR_r)_i$ more effectively reduces the displacements and drifts of only the upper stories compared to the traditional TMD and it significantly mitigates the problematic drift amplification in the upper floors. The optimal TMD associated with the minimum average $(D_r)_i$ more effectively reduces the displacements and drifts of all stories compared to the traditional TMD, and its performance in addressing the problematic drift amplification in the upper floors is acceptable but less than that of the first optimal TMD.

- A comparison of the proposed TMD with the optimal TMDs recommended in previous studies demonstrated that, while both configurations perform comparably in elastic structures, the proposed TMD achieves significantly superior performance in structures exhibiting nonlinear behavior.

- The improved stiffness-based tuning strategy developed in this study was applied to a Tuned Structural Mass Damper (TSMD) configuration, in which a portion of the top floor mass is utilized as the TMD mass. This combined approach proved particularly effective, achieving comparable performance to traditional TMDs with added mass while eliminating the need for additional structural weight.

- In nonlinear MDOF systems, the TSMD with reduced stiffness maintained its effectiveness compared to the traditional TMD. The results showed that the performance of the TSMD in the lower stories is similar to that of the traditional TMD. However, the TSMD was able to reduce drift ratios in the upper stories more effectively, while the traditional TMD increased drifts in the upper stories, especially at the roof. These findings collectively demonstrate that while traditional TMDs have limitations, particularly in nonlinear structures, carefully optimized systems (especially those employing structural mass) can provide substantial improvements in seismic performance without the drawbacks of added mass or excessive retrofitting costs.

### 5.2. Limitations and Future Work

While the present study provides a comprehensive investigation of the proposed stiffness-based tuning strategy, several important limitations should be acknowledged that also suggest clear directions for future research. First, it is noteworthy that the nonlinear behavior of the structures was modeled using a bilinear hysteretic model, which does not capture stiffness degradation, strength deterioration, and pinching effects. Therefore, future studies should extend the proposed strategy to structures governed by more advanced hysteretic models. Second, a further limitation is that soil–structure interaction (SSI) effects were not considered. Because SSI can significantly alter the dynamic response of structures on soft soils, its influence on the proposed TMD and TSMD configurations is an essential topic for future investigation. Third, it should be stressed that only a single TMD placed at the top floor was considered in the MDOF analyses. A systematic exploration of alternative TMD placements and the use of multiple tuned mass dampers (MTMDs) distributed along the building height could yield valuable insights into optimal system arrangements. Fourth, it is also important to note that the present study employed simplified SDOF and shear-building MDOF models. Future work should therefore investigate the proposed approach using detailed three-dimensional finite element models subjected to a broader range of earthquake records in order to facilitate practical implementation.

## 6. References


[1] H. Frahm, Device for damping vibrations of bodies, U.S. Patent No. 989958, 1911.

[2] J.P. Den Hartog, Mechanical vibrations, Courier Corporation, 1985.

[3] R.J. McNamara, Tuned mass dampers for buildings, Journal of the Structural Division, 103(9) (1977) 1785–1798.

[4] F. Sadek, B. Mohraz, A.W. Taylor, R.M. Chung, A method of estimating the parameters of tuned mass dampers for seismic application, Earthquake Engineering Structural Dynamics, 26(5) (1997) 617–635.

[5] G.B. Warburton, Optimum absorber parameters for various combinations of response and excitation parameters, Earthquake Engineering Structural Dynamics, 10(3) (1982) 381–401.

[6] A.Y.T. Leung, H. Zhang, Particle swarm optimization of tuned mass dampers, Engineering Structures, 31(3) (2009) 715–728.

[7] H. Zhang, L. Zhang, Tuned mass damper system of high-rise intake towers optimized by improved harmony search algorithm, Engineering Structures, 138 (2017) 270–282.

[8] S. Etedali, M. Akbari, M. Seifi, MOCS-based optimum design of TMD and FTMD for tall buildings under near-field earthquakes including SSI effects, Soil Dynamics and Earthquake Engineering, 119 (2019) 36–50.

[9] J. Love, T. Haskett, B. Morava, Effectiveness of dynamic vibration absorbers implemented in tall buildings, Engineering Structures, 176 (2018) 776–784.

[10] O. Araz, Optimization of three-element tuned mass damper based on minimization of the acceleration transfer function for seismically excited structures, Journal of the Brazilian Society of Mechanical Sciences and Engineering, 44(10) (2022) 459.

[11] B. Ozturk, H. Cetin, E. Aydin, Optimum vertical location and design of multiple tuned mass dampers under seismic excitations, Structures, 41 (2022) 1141–1163.

[12] H. Jafarinia, K. Ostad-Ali-Askari, Optimum setting parameters of multiple tuned mass damper for passive control of structures using cuckoo algorithm, Iranian Journal of Science and Technology, Transactions of Civil Engineering, 48(3) (2024) 1483–1496.

[13] D.-P.N. Kontoni, A.A. Farghaly, Seismic control of vertically and horizontally irregular steel high-rise buildings by tuned mass dampers including SSI, Asian Journal of Civil Engineering, 25(2) (2024) 1995–2014.

[14] Z. Lu, D. Wang, P. Li, Comparison study of vibration control effects between suspended tuned mass damper and particle damper, Shock and Vibration, 2014(1) (2014) 903780.

[15] Q. Wu, W. Zhao, W. Zhu, R. Zheng, X. Zhao, A tuned mass damper with nonlinear magnetic force for vibration suppression with wide frequency range of offshore platform under earthquake loads, Shock and Vibration, 2018(1) (2018) 1505061.

[16] Y.-j. Kang, L.-y. Peng, Optimization design and damping effect analysis of large mass ratio tuned mass dampers, Shock and Vibration, 2019(1) (2019) 8376781.

[17] M. De Angelis, A. Giaralis, F. Petrini, D. Pietrosanti, Optimal tuning and assessment of inertial dampers with grounded inerter for vibration control of seismically excited base-isolated systems, Engineering Structures, 196 (2019) 109250.

[18] L.A. Lara-Valencia, Y. Farbiarz-Farbiarz, Y. Valencia-González, Design of a tuned mass damper inerter (TMDI) based on an exhaustive search optimization for structural control of buildings under seismic excitations, Shock and Vibration, 2020(1) (2020) 8875268.

[19] H. Gao, C. Wang, C. Huang, W. Shi, L. Huo, Development of a Frequency-Adjustable Tuned Mass Damper (FATMD) for Structural Vibration Control, Shock and Vibration, 2020(1) (2020) 9605028.

[20] C. Masnata, A. Di Matteo, C. Adam, A. Pirrotta, Assessment of the tuned mass damper inerter for seismic response control of base-isolated structures, Structural Control and Health Monitoring, 28(2) (2021) e2665.

[21] O. Araz, Optimization of tuned mass damper inerter for a high-rise building considering soil-structure interaction, Archive of Applied Mechanics, 92(10) (2022) 2951–2971.

[22] B. Besharatian, H.T. Riahi, R. Garcia, I. Hajirasouliha, A practical optimisation method for friction tuned mass dampers in multi-storey buildings subjected to earthquake excitations, Soil Dynamics and Earthquake Engineering, 184 (2024) 108857.

[23] A. Das, A. Banerjee, D.R. Sahoo, V. Matsagar, Inerter-based tuned mass dampers for response control of multi-degree-of-freedom structures subjected to wind and earthquake excitations, Structure and Infrastructure Engineering, 22(4) (2026) 624–637.

[24] S. Bagheri, V. Rahmani-Dabbagh, Seismic response control with inelastic tuned mass dampers, Engineering Structures, 172 (2018) 712–722.

[25] T.A. Sakr, Vibration control of buildings by using partial floor loads as multiple tuned mass dampers, Housing and Building National Research Center Journal, 13(2) (2017) 133–144.

[26] H. Anajafi, R.A. Medina, Comparison of the seismic performance of a partial mass isolation technique with conventional TMD and base-isolation systems under broad-band and narrow-band excitations, Engineering Structures, 158 (2018) 110–123.

[27] A. Manchalwar, S. Bakre, Vibration control of structure by top base isolated storey as tuned mass damper, International Journal of Dynamics and Control, 8(3) (2020) 963–972.

[28] M.H. Stanikzai, S. Elias, V.A. Matsagar, A.K. Jain, Seismic response control of base-isolated buildings using multiple tuned mass dampers, The Structural Design of Tall and Special Buildings, 28(3) (2019) e1576.

[29] A. Di Matteo, C. Masnata, A. Pirrotta, Hybrid passive control strategies for reducing the displacements at the base of seismic isolated structures, Frontiers in Built Environment, 5 (2019) 132.

[30] R. Mohammadi, A. Ziarani, Passive control using optimum tuned mass damper and its effectiveness in a nonlinear structure, Sharif Journal of Civil Engineering, 2(2/2) (2016) 107–115.

[31] M. Khatibinia, S. Akbari, H. Yazdani, S. Gharehbaghi, Damage-based optimal control of steel moment-resisting frames equipped with tuned mass dampers, Journal of Vibration and Control, 30(3-4) (2024) 659–672.

[32] M. Roozbahan, G. Turan, An improved passive tuned mass damper assisted by dual stiffness, Structures, 50 (2023) 1598–1607.

[33] M.A. Shahraki, R. Kamgar, H. Heidarzadeh, Assessing the seismic behavior of structures controlled with a novel elastoplastic-tuned mass damper inerter considering the effects of soil-structure interactions, Structures, 57 (2023) 105265.

[34] I.S. Code, Iranian code of practice for seismic resistant design of buildings, Standard No. 2800, Building and Housing Research Center, Iran, 2015.

[35] FEMA, Improvement of nonlinear static seismic analysis procedures (FEMA 440), Federal Emergency Management Agency, Washington, D.C., 2005.

[36] PEER, PEER Ground Motion Database, Pacific Earthquake Engineering Research Center, University of California, Berkeley, available at: https://ngawest2.berkeley.edu/

[37] H. Naderpour, A. SoltaniMatin, A. Kheyroddin, P. Fakharian, N. Ezami, Optimizing seismic performance of tuned mass dampers at various levels in reinforced concrete buildings, Buildings, 14(8) (2024) 2443.